IOPscience iopscience.iop.org

Home Search Collections Journals About Contact us My IOPscience

Photoluminescence of ZnO thin films on Si substrate with and without ITO buffer layer

This article has been downloaded from IOPscience. Please scroll down to see the full text article.

2006 J. Phys. D: Appl. Phys. 39 471

(http://iopscience.iop.org/0022-3727/39/3/008)

View the table of contents for this issue, or go to the journal homepage for more

Download details:
IP Address: 202.127.206.107
The article was downloaded on 30/06/2010 at 09:15

Please note that terms and conditions apply.

INSTITUTE OF PHYSICS PUBLISHING JOURNAL OF PHYSICS D: APPLIED PHYSICS

J. Phys. D: Appl. Phys. **39** (2006) 471–476 doi:10.1088/0022-3727/39/3/008

Photoluminescence of ZnO thin films on Si substrate with and without ITO buffer layer

X M Teng, H T Fan, S S Pan, C Ye and G H Li[1]

Key Laboratory of Materials Physics, Anhui Key Laboratory of Nanomaterials and Nanostructure, Institute of Solid State Physics, Chinese Academy of Sciences, Hefei 230031, People's Republic of China

E-mail: ghli@issp.ac.cn

Received 27 September 2005, in final form 15 November 2005
Published 20 January 2006
Online at stacks.iop.org/JPhysD/39/471

Abstract
Photoluminescence (PL) properties of ZnO thin films on Si substrate with and without an indium tin oxide (ITO) buffer layer, prepared under different oxygen partial pressures in the sputtering gas, were studied. It was found that PL characteristics of ZnO thin films depend on oxygen partial pressure and substrate, and the PL peak in the ultraviolet region has a strong red-shift with increasing excitation intensity on the glass and Si substrates with the ITO buffer layer, and the PL intensity increases with the increasing measuring cycle. Enhanced luminescence efficiency of ZnO thin films on the substrates with ITO buffer layer measured at different cycles can be obtained by thermal annealing.

1. Introduction

ZnO is a wide band-gap semiconductor that possesses a versatile combination of interesting optical, electrical and magnetic properties. The ZnO thin film plays an important role in various technological domains, such as transparent conducting thin films/electrodes in display devices and solar cells, surface and bulk acoustic wave devices and acoustic optical devices and light-emitting diodes and laser diodes, due to its large bond strength, good optical quality, extreme stability of excitons and excellent piezoelectric properties [1–4]. Another advantage of ZnO relative to other materials is its low price, placing it as a high potential candidate for industrial applications. Thus, accurate knowledge of the structural and optical properties of the ZnO thin film is indispensable for the design and analysis of various optical and optoelectronic devices.

The optical and physical properties of ZnO thin films grown by a variety of deposition methods [5–10] are affected by the substrate temperature, substrate material, sputtering conditions and annealing treatment [10–16]. Moreover, the selection of substrate is vital for the growth of the ZnO thin film because the match in lattice parameters and crystal structure between the film and substrate strongly affect the crystal growth behaviour of the films [8].

In fact, the growth of high-quality thin film on Si substrate is a key technology for the realization of optoelectronic integrated circuits. However, due to the large lattice mismatch between ZnO and Si, the large number of dislocations limit the material quality and consequently prevent practical use. In order to overcome this problem, several research groups used a homo-buffer layer on sapphire substrates grown by metal-organic chemical vapour deposition and magnetron sputtering at low temperatures and obtained enhanced structural and optical properties [17, 18]. Indium tin oxide (ITO) glass substrate has many excellent properties, such as being electrically conductive and optically transparent, high Vis–Nir light transmission, uniform transmission homogeneity and reflection in the infrared range. ZnO thin films grown on ITO glass substrates exhibit good crystal quality duo to a small lattice mismatch (3%) between the neighbouring oxygen–oxygen (O–O) distance on the closet-packed [111] plane of ITO and [0001] plane of ZnO [19–22]. On the other hand, there are O dangling bonds on the ITO layer surface, which are beneficial for the initial nucleation of ZnO and the subsequent growth of a high quality thin film.

To utilize the ZnO thin film for large-scale optoelectronic devices, it is required to have a better understanding of the

[1] Author to whom any correspondence should be addressed.

factors controlling the optical properties of ZnO thin films. In this paper, the influence of the ITO buffer and oxygen partial pressure on the structural and Photoluminescence (PL) properties of ZnO thin films on different substrates were reported, and some abnormal PL features were found for the first time.

2. Experimental procedure

ZnO thin films were grown on n-[100] Si with and without the ITO buffer layer and ITO glass substrates from a ZnO target (99.999%) using an rf magnetron sputter system at a constant substrate temperature of 400 °C. The chamber was first pumped to a base vacuum better than 5×10^{-6} Pa and then filled with a mixture of Ar and O_2, in which the oxygen partial pressure, P_{O_2} [$O_2/(O_2 + Ar)$], ranged from 0% to 100%. The sputtering was carried out at a constant gas working pressure of 1 Pa, rf power of 80 W and bias voltage of 50 V. The ITO buffer layer was deposited at a constant gas working pressure of 1 Pa, rf power of 100 W and bias voltage of 50 V. The as-grown ITO layer is amorphous, with a thickness of about 50 nm. Since the growth rate of the ZnO thin film decreases with increasing P_{O_2}, different growth times were used under different oxygen partial pressures in order to obtain ZnO thin films with approximately the same thickness. The as-grown ZnO thin films have a thickness of about 200±30 nm as determined by spectroscopic ellipsometry (UVISEL Jobin-Yvon). Some of the samples (ZnO thin film on Si substrate with ITO buffer layer) were post-annealed at different temperatures in air, and a slow cooling rate of about 2 K min^{-1} was maintained to avoid stress within the ZnO thin films.

X-ray diffraction (XRD, Philips PW 1700x with Cu Kα radiation), field-emission scanning electron microscopy (FE-SEM, FEI Sirion 200) and atomic force microscopy (AFM) were used to study the crystalline structure and morphology of ZnO thin films. Optical transmission spectra were measured using a Carry 5E spectrometer in the wavelength range of 300–1200 nm. PL spectra were measured on a LABRAM-HR spectrometer (He-Cd laser) with an excitation wavelength of 325 nm and excitation intensity of 2000 W cm^{-2} at room temperature.

3. Results and discussion

To optimize the growth conditions, the influence of P_{O_2} on the structure of as-grown ZnO thin films was studied first. Figure 1 shows the XRD patterns of ZnO thin films deposited on ITO glass and Si substrates with different P_{O_2}. Only one strong peak attributed to the diffraction of the [0002] plane of the hexagonal wurtzite ZnO can be observed. It suggests that the as-grown ZnO thin films exhibit [0002] preferential orientation with the *C*-axis perpendicular to the substrate. Note that the peak intensity increases with increasing P_{O_2} and then decreases with further increasing P_{O_2}. This intensity variation is not due to the change in thickness of the films. The initial increase may result from the improved stoichiometry of the films, associated with the incorporation of oxygen at oxygen vacancies. However, P_{O_2} beyond the equilibrium value might worsen the stoichiometry of the films by introducing interstitial oxygen or zinc vacancies.

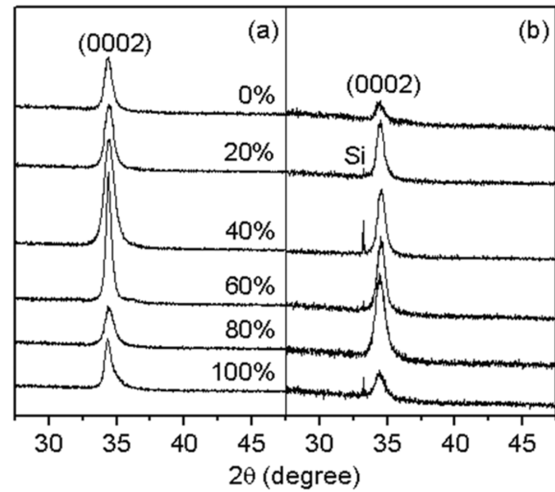

Figure 1. XRD patterns of ZnO thin films deposited on (*a*) ITO glass and (*b*) Si substrate with different oxygen partial pressures.

Table 1. Lattice parameters and strain of ZnO thin films deposited on different substrates.

Substrate	ITO	Si
O_2 partial pressure	60%	80%
Peak position (2θ)	34.42 °	34.45 °
FWHM (°)	0.12 °	0.6 °
Lattice constant (Å)	5.211	5.201
Strain, ε_{zz} (%)	0.085%	−0.11%

Table 1 shows the properties of ZnO thin films on the ITO glass and Si substrates at the optimized P_{O_2}. One can see that the optimized P_{O_2} for the ZnO thin film grown on ITO glass is lower than that on the Si substrate, possibly due to the rich O dangling bond on ITO surface. The full width at half maximum (FWHM) of the former is smaller than the latter. All this indicates that ITO appears to be a suitable buffer layer for the occurrence of the preferential orientation of the good quality ZnO thin film, which is due to the small lattice mismatch between ITO and ZnO and the ITO good surface properties as mentioned above. It is also apparent that the 2θ value of [0002] peak shifts slightly from the standard value ($2\theta = 34.43$ °) [23], indicating the formation of defects in the as-grown thin films. This is because a shift in the 2θ value arises from an increase of the local strain around the impurity or lattice defects [24]. Note that the strain is tensile between ZnO and ITO and is compressive between ZnO and Si.

The surface roughness of ZnO thin films (extracted from AFM data) also depends on P_{O_2}, as shown in figure 2. The surface roughness of ZnO thin films on the Si substrate decreases with increasing P_{O_2}, after reaching the minimum value at about 80% P_{O_2} and then slightly increases. That on the ITO glass substrate drops rapidly at about 20% P_{O_2}, after reaching the minimum value at 40% P_{O_2} and then nearly stays constant with further increasing P_{O_2}. In this case, the presence of O_2 not only saturates any uncompensated bonds reducing the bulk defects but also reduces the growth rate due to the lower mass of the oxygen ion. This is attributed to the good crystallization and small lattice mismatch between the ZnO and ITO buffer layer. At the surface of the initial grown thin

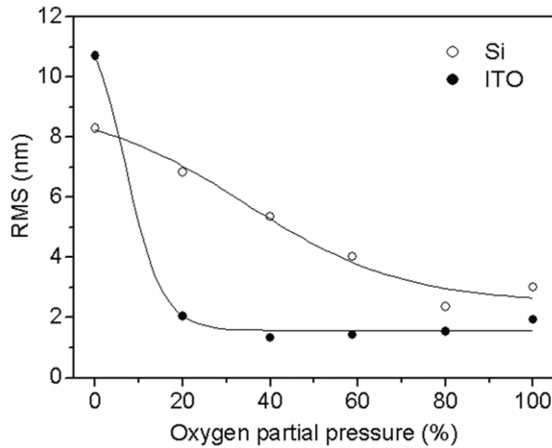

Figure 2. Roughness of ZnO thin films as a function of oxygen partial pressure for different substrates.

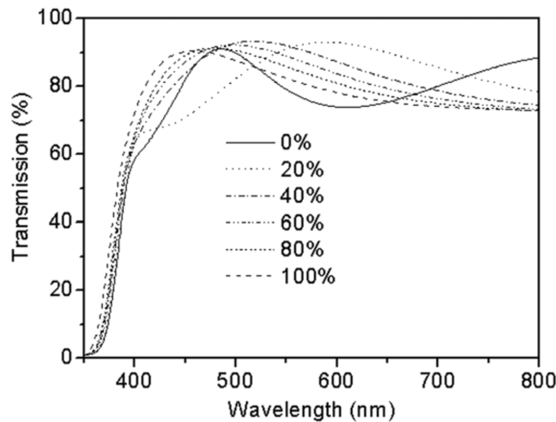

Figure 3. Optical transmittance spectra of ZnO thin films on ITO glass substrate with different oxygen partial pressures.

film, it is thus easy for the crystallization and densification to begin in the presence of the dangling bond.

Transmission spectra of ZnO thin films grown on the ITO glass substrate with different P_{O_2} are shown in figure 3. The film stoichiometry was indirectly evaluated by observing the optical transmittance spectra. All the thin films exhibit a high transmittance (about 90%) in the visible region and show a sharp fundamental absorption edge at about 380 nm. The transmission is minimum for the film grown in pure Ar, and the peak value increases slightly and subsequently decreases with increasing P_{O_2}. The different degrees of interference in the transmittance spectra might be due to the slight difference in film thickness.

Figure 4 shows the room temperature PL spectra of ZnO thin films with different P_{O_2}. The PL spectra, being similar to those reported by others [25], are featured by a strong PL near the ultraviolet region (UV–PL) and a weak defect-related emission in the visible region. The UV–PL band on ITO glass is situated at about 395 nm (see figure 4(*a*)), and the intensity of it firstly increases with increasing P_{O_2} due to the increased oxygen stoichiometric, reaches the maximum at 60% P_{O_2} and then decreases, whilst the PL peak position slightly shifts to longer wavelength. In the case of the Si substrate the signal peaks at about 380 nm (see figure 4(*b*)), the PL

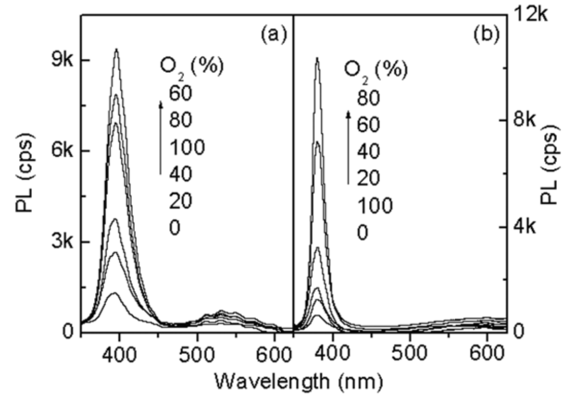

Figure 4. PL spectra of ZnO thin films grown on (*a*) ITO glass and (*b*) Si substrate with different oxygen partial pressures.

intensity also increases with increasing P_{O_2} and reaches the maximum at 80% P_{O_2} and then decreases again, and the peak position almost does not change. This trend is consistent with the XRD measurement. Enhanced stoichiometry of ZnO thin films with the increased P_{O_2} will have the stronger UV light emission. However, the further increase in P_{O_2} will degrade the crystallization quality, and, consequently, the UV light emission.

The sharp UV emission peak around 380 nm of the ZnO thin film on the Si substrate is due to the excitonic related recombination. Due to the large exciton binding energy of ZnO (about 60 meV), excitons have been observed at room temperature. It has also been reported that thermal energy at room temperature may be enough to release bound excitons because the binding energy of bound excitons is only a few millielectronvolt [26]. The exciton level at 380 nm of ZnO thin films on Si substrate is very close to the typically reported free exciton peak position [27, 28]. The emission intensity is determined by the radiative and nonradiative transition, and the nonradiative transition is generally induced by crystal imperfections, such as oxygen vacancies in ZnO thin films deposited by sputtering. These defects produce various nonradiative centres and reduce emission intensity.

The influence of excitation intensities on UV–PL of ZnO thin films on ITO glass (60% P_{O_2}) is shown in figure 5(*a*). It can be observed that UV emission intensity increases with the increase of the excitation intensity, which is in agreement with the previously reported result for ZnO nanowires [29], while the peak position of the emission band shifts from 383 (3.24 eV) to 395 nm (3.14 eV) by 100 meV, and this red-shift is different from the results observed in semiconductor quantum dots and quantum well. Since the exciton density increases with excitation intensity, different exciton-related emissions might occur. In the intermediate density regime, biexcitonic, exciton–exciton and exciton–carrier emissions may be observed. Biexcitonic emissions are only observed at cryogenic temperatures. At higher temperatures exciton ionization increases the free carrier densities, and thus an increased probability of exciton–carrier emission. At high excitation intensities, the dominated peak can be attributed to electron hole plasma recombination shifted by band gap renormalization [30]. Since the energy shift with excitation intensity is too high to attribute this transition completely

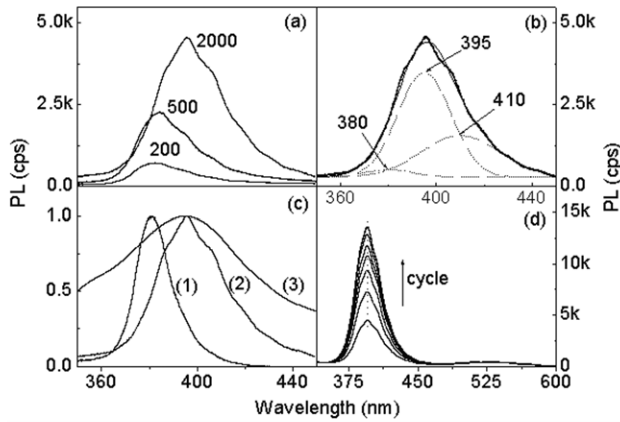

Figure 5. PL spectra of ZnO thin films on ITO glass (60% P_{O_2}): (*a*) excited with different excitation intensities (W cm^{-2}), (*b*) Gaussian fitting of the top PL band in (*a*), (*c*) normalized PL spectra of curve (1) ZnO thin film on Si substrate, curve (2) ZnO thin film on ITO substrate and (3) ITO substrate, (*d*) excited at different measuring cycles.

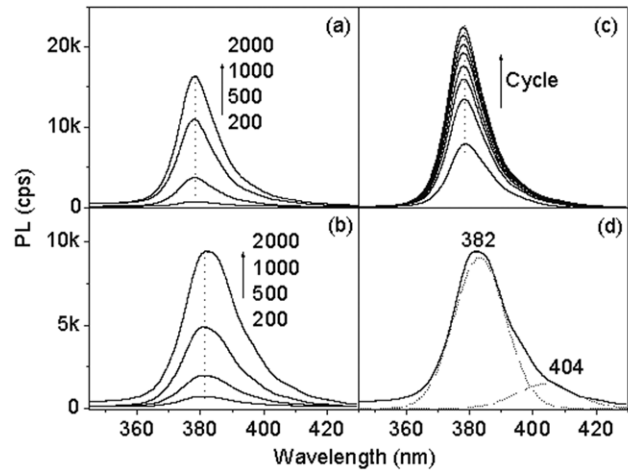

Figure 6. PL spectra of ZnO thin films on Si substrate (60% P_{O_2}): (*a*) without and (*b*) with ITO buffer excited with different excitation intensities (W cm^{-2}), (*c*) with ITO buffer excited at different measuring cycles and (*d*) Gaussian fitting of the top PL band in (*b*).

to exciton emission, the transition may be also come from the recombination located at the interface between ZnO and the ITO glass substrate. The Gaussian fitting of the UV–PL band gives three peaks situated, respectively, at 380, 395 and 410 nm, as shown in figure 5(*b*). It is evident that at high excitation intensity, the spectrum is dominated by the low-energy component, i.e. the peak at 395 nm, but low excitation intensity is favourable for the high-energy component, i.e. the peak at 380 nm. The emission at 3.1 eV (400 nm) has been frequently observed in natural silica and oxygen-deficient silica glass [31, 32]. In the present study the PL peak from the ITO layer is situated at 395 nm with a wider FWHM, as shown in figure 5(*c*). Sekiguchi *et al* [33] have observed the blue emission at about 413 nm in ZnO thin films grown under an oxygen rich condition by the chemical vapour deposition method and attributed the PL to the possible existence of cubic ZnO, which might exist near the substrate interface in ZnO thin films [34]. Because there is no evidence for the existence of cubic ZnO from the XRD analysis in our samples, the O dangling bonds on the ITO surface layer or the interface between substrate and ITO might contribute to the anomalous emission (410 nm, 3.0 eV).

Figure 5(*d*) shows the PL spectra of the ZnO thin film on the ITO glass substrate (60% P_{O_2}) measured at different cycles with the same excitation intensity (2000 W cm^{-2}). One can see that the intensity of the UV–PL peak increases with the measuring cycle and after about eight cycles nearly reaches the saturated level, while that in the visible wavelength almost does not change. Laser annealing has frequently been used in the semiconductor industry for dopant activation and defects elimination. In the present study the laser irradiation during the measurement can be regarded as a laser annealing, which can decrease the nonradiative point and extended defects in the ZnO thin film, which thus increases the luminescence efficiency of the thin films at the following cycles. Note that such laser annealing effect can enhance both the peak and integrated PL efficiency at the UV region, up to a factor of 2–3 compared with the as-grown thin films, without any spectral shift of the peak position.

Figure 6(*a*) shows UV–PL spectra of the ZnO thin film on Si substrate (60% P_{O_2}) excited with different excitation intensities. Note that the emission intensity almost linearly increases with the increase of excitation intensity and the peak position at 379 nm has no shift. Further PL measurements indicate that the emission intensity has no change with the increasing measuring cycles under the same excitation intensity (2000 W cm^{-2}). Figure 6(*b*) shows UV–PL spectra of the ZnO thin film on Si substrate with the ITO buffer layer (60% P_{O_2}) excited with different excitation intensities. The emission intensity also linearly increases and the peak position at 382 nm slightly shifts to long wavelength with increasing excitation intensity. It is seen that the peak position of the ZnO thin film on Si substrate with the ITO buffer slightly shifts to longer wavelength compared with that without the ITO buffer layer, see figures 6(*a*) and (*b*). The Gaussian fitting of the PL band gives two peaks situated, respectively, at 382 and 404 nm, see figure 6(*c*). As mentioned above, the peak at 382 nm corresponds to the emission from ZnO. The origin of the PL peak at 404 nm (3.06 eV) will be discussed later. Figure 6(*d*) shows the PL spectra of the ZnO thin film on Si substrate with the ITO buffer layer (60% P_{O_2}) measured at different cycles with the same excitation intensity (2000 W cm^{-2}). The intensity of UV–PL peak also increases with the increasing measuring cycle and even after about eight cycles does not reach the saturated level, while the emission in the visible wavelength does not change. It is worth noting that the PL intensity of the ZnO thin film on Si substrate with the ITO buffer layer is lower than that without the ITO buffer layer; however, after eight measuring cycles, the PL intensity of the former is higher than the later.

In the schematic energy levels of the defects in the ZnO thin film obtained by the full-potential linear muffin-tin orbital method [35] (not shown here), the energy interval from the top of the valence band to the Zn_i level (interstitial zinc, 2.9 eV) is nearly in accord with the energy of the Gaussian fitting peak at 410 nm (3.0 eV) of the ZnO thin film on ITO glass shown in figure 5(*b*). The energy interval from the bottom of the conduction band to the V_{Zn} level (non-ionized vacancies

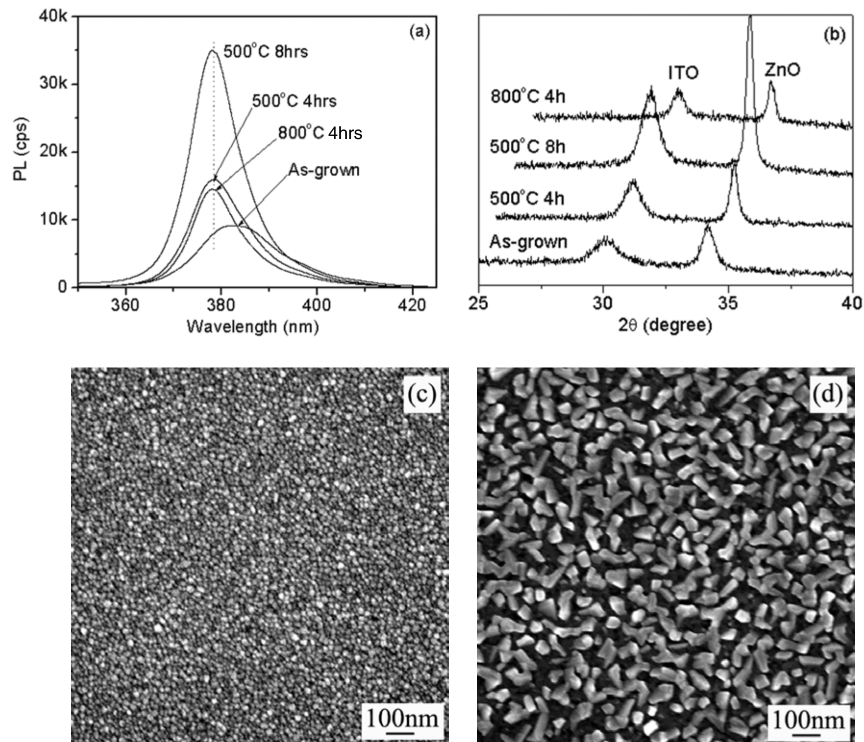

Figure 7. (*a*) PL spectra and (*b*) XRD patterns of ZnO thin films on Si with ITO buffer layer annealed at different temperatures and time. FE-SEM images of ZnO thin films on Si with ITO buffer layer annealed at (*c*) 500 °C for 4 h and (*d*) 800 °C for 4 h.

of zinc, 3.06 eV) is exactly consistent with the energy of the Gaussian fitting peak at 404 nm (3.06 eV) from the ZnO thin film on Si substrate with the ITO buffer layer in figure 6(*d*). Note that these two peaks disappeared from the ZnO thin film on glass and Si substrates without the ITO buffer layer.

Figure 7(*a*) shows the PL spectra of ZnO thin films on Si substrate with the ITO buffer at different annealing temperatures and time. As expected, the emission intensity increases and the peak position shifts to the short wavelength with increasing annealing time. The PL intensity of the ZnO thin film annealed at 800 °C for 4 h is lower than that annealed at 500 °C for 4 h but still higher than the as-grown one. The higher temperature annealing often causes the degradation of the crystal quality and thus has the opposite effect of lowering the luminescence efficiency. Post-growth annealing could improve the emission efficiency due to the decrease of the nonradiative defects and the increase of ZnO grain size [12]. With longer annealing time at 500 °C, the FWHM becomes smaller, and peak intensity becomes stronger compared with the as-grown one. But the diffraction intensity decreases when annealed at 800 °C for 4 h, which might be due to the inter-diffusion effect between ITO and ZnO, as evidenced by the shift of the XRD peaks. FE-SEM observations indicate that after annealing at 500 °C for 4 h, ZnO grain size slightly increases in comparison with the as-grown one, see figure 7(*c*). But after annealing at 800 °C for 4 h the grain size increased to about 60–100 nm and the grains had a rod-like structure, see figure 7(*d*). The emission intensity of ZnO thin films on Si substrate with ITO buffer layer annealed at 500 °C for 4 h increases with the measuring cycle and has the same feature as that shown in figure 6(*c*), while that annealed at 500 °C for 8 h does not change. But when annealed at 800 °C for only 4 h, the PL intensity only slightly increases with the measuring cycle. These results indicate that the annealing treatment at 500 °C for only 4 h is not enough to obtain the stoichiometric ZnO thin film; more than 8 h is needed.

The above results clearly indicate that the ITO buffer layer plays an important role in the PL characteristics of ZnO thin films, particularly, the PL peak position shifts with excitation laser intensity and PL intensity increases with the measuring cycle. Enhanced emission efficiency of the ZnO thin film on Si substrate with the ITO buffer layer with laser measuring cycles is closely related to the thermal effect.

In conclusion, *C*-crystal axis orientated ZnO thin films with high optical transmission are prepared by rf magnetron sputtering on a ITO glass substrate and on Si substrate with and without a ITO buffer layer. The optimized sputtering P_{O_2} of ZnO thin films on Si substrate is about 80%, while that on the ITO glass and Si substrate with the ITO buffer layer is about 60%. Both the surface roughness and grain size of ZnO thin films decrease in the presence of the ITO buffer layer. The UV–PL characteristics of ZnO thin films clearly depend on the substrate and P_{O_2}, and that on the ITO glass substrate grown at 60% P_{O_2} has the maximum PL intensity, while that on Si substrate grown at 80% P_{O_2} has the maximum PL intensity. The UV–PL peak intensity of the ZnO thin film on the ITO glass substrate nonlinearly increases and the peak position shifts to long wavelength with the increase of excitation intensity, while that on the Si substrate almost linearly increases, and the PL peak position has no shift with the increase of excitation intensity. The intensity of UV–PL peak increases with the measuring cycle for the ZnO thin film on the ITO glass and Si substrate with the ITO buffer layer, but has no change on the Si substrate without the ITO buffer layer. The blue emission at

about 410 nm of the ZnO thin film on ITO glass is considered to be due to the transition from the top of the valence band to the Zn_i level (2.9 eV), and the blue emission at about 404 nm of the ZnO thin film on the Si substrate with the ITO buffer layer is linked to the transition from the bottom of the conduction band to the V_{Zn} level (3.06 eV). Proper annealing treatment can enhance the PL intensity of ZnO thin films on the Si substrate with the ITO buffer layer. It is concluded that the ITO buffer layer has a critical effect on the PL of ZnO thin films, and enhanced emission efficiency of ZnO thin films on the substrates with the ITO buffer layer measured at different cycles is considered due to the thermal effect.

Acknowledgment

This work was supported by the National Natural Science Foundation of China (No:10474098).

References

[1] Saeki H, Matsui H, Kawai T and Tabata H 2004 *J. Phys.: Condens. Matter* **16** S5533
[2] Zhang X Q, Tang Z K, Kawasaki M, Ohtomo A and Koinuma H 2003 *J. Phys.: Condens. Matter* **15** 5191
[3] Mahmood F S, Gould R D and Salih M H 1995 *Thin Solid Films* **270** 376
[4] Gorla C R, Emanetoglu N W, Liang S, Mayo W E, Lu Y, Wraback M and Shen H 1999 *J. Appl. Phys.* **85** 2595
[5] He H P, Wang Y X and Zou Y M 2003 *J. Phys. D: Appl. Phys.* **36** 2972
[6] Zhao G L, Lin B X, Hong L, Meng X D and Fu Z X 2004 *Chin. Phys. Lett.* **21** 1381
[7] Wang X Q, Du G T, Gu C Z, Jia J K, Li X J, Yan F W, Ong H C, Liu D L and Yang S R 2002 *J. Phys. D: Appl. Phys.* **35** L74
[8] Ghosh R, Basak D and Fujihara S 2004 *J. Appl. Phys.* **96** 2689
[9] Yu Q X, Xu B, Wu Q H, Liao Y, Wang G Z and Fang R C 2003 *Chin. Phys. Lett.* **20** 2235
[10] Mehan N, Gupta V, Sreenivas K and Mansingh A 2004 *J. Appl. Phys.* **96** 3134
[11] Zhi Z Z, Liu Y C, Li B S, Zhang X T, Lu Y M, Shen D Z and Fan X W 2003 *J. Phys. D: Appl. Phys.* **36** 719
[12] Jeong S H, Kim J K and Lee B T 2003 *J. Phys. D: Appl. Phys.* **36** 2017
[13] Kim T W, Kwack K D, Kim H K, Yoon Y S, Bahang J H and Park H L 2003 *Solid State Commun.* **127** 635
[14] Kim I S, Jeong S H, Kim S S and Lee B T 2004 *Semicond. Sci. Technol.* **19** L29
[15] Liu Y L, Liu Y C, Yang H, Wang W B, Ma J G, Zhang J Y, Lu Y M, Shen D Z and Fan X W 2003 *J. Phys. D: Appl. Phys.* **36** 2705
[16] David T, Goldsmith S and Boxman R L 2005 *J. Phys. D: Appl. Phys.* **38** 2407
[17] Jeong S H, Kim I S, Kim S S, Kim J K and Lee B T 2004 *J. Cryst. Growth* **264** 110
[18] Jeong S H, Kim I S, Kim J K and Lee B T 2004 *J. Cryst. Growth* **264** 327
[19] Yi C H, Yasui I and Shigesato Y 1995 *Japan. J. Appl. Phys.* **34** 1639
[20] Lee S Y and Park B O 2005 *Thin Solid Films* **484** 184
[21] Jeong S H, Lee S B and Boo J H 2004 *Curr. Appl. Phys.* **4** 655
[22] Wang Z J, Zhang H M, Wang Z J, Zhang L G and Yuan J S 2003 *J. Mater. Res* **18** 151
[23] King S, Gardeniers J G E and Boyd I W 1996 *Appl. Surf. Sci.* **96–98** 811
[24] Ohkawa Y, Mitsuyu T and Yamazaki O 1987 *J. Appl. Phys.* **62** 3216
[25] Cho S L, Ma J, Kim Y K, Sun Y, Wong G K L and Ketterson J B 1999 *Appl. Phys. Lett.* **75** 2761
[26] Hichou A El, Kachouane A, Bubendorff J L, Addou M, Ebothe J, Troyon M and Bougrine A 2004 *Thin Solid Films* **458** 263
[27] Chen Y F, Bagnall D M, Koh H J, Park K T, Hiraga K, Zhu Z and Yao T 1998 *J. Appl. Phys.* **84** 3912
[28] Bagnall D M, Chen Y F, Shen M Y, Zhu Z, Goto T and Yao T 1998 *J. Cryst. Growth* **184/185** 605
[29] Lyu S C, Zhang Y, Ruh H, Lee H J, Shim H W, Suh E K and Lee C J 2002 *Chem. Phys. Lett.* **363** 134
[30] Bagnall D M, Chen Y F, Zhu Z, Yao T, Shen M Y and Goto T 1998 *Appl. Phys. Lett.* **73** 1038
[31] Cannas M, Barbera M, Boscaino R, Collura A, Gelardi F M and Varisco S 1999 *J. Non-Cryst. Solids* **245** 190
[32] Sakurai Y 2000 *J. Non-Cryst. Solids* **271** 218
[33] Sekiguchi T, Haga K and Inaba H 2000 *J. Cryst. Growth* **214/215** 68
[34] Xin Y, Brown P D, Boothroyd C B, Preston A R, Humphreys C J, Cheng T S, Foxon C T, Andrianov A V and Orton J W 1996 *Mater. Res. Soc. Symp. Proc.* **423** 311
[35] Sun Y M 2000 *PhD Thesis* University of Science and Technology of China